

H. X. Zong · C. J. Cong · L. N. Wang ·
G. H. Guo · Q. Y. Liu · K. L. Zhang

Synthesis and electrochemical properties of yttrium-doped LiMn_{0.98}Y_{0.02}O₂ for lithium secondary batteries

Received: 5 November 2005 / Revised: 14 November 2005 / Accepted: 28 November 2005 / Published online: 3 January 2006
© Springer-Verlag 2006

Abstract Yttrium-doped lithium manganese oxide (LiMn_{0.98}Y_{0.02}O₂) was prepared by ion exchange of lithium for sodium in NaMn_{0.98}Y_{0.02}O₂ precursors obtained by using rheological phase reaction method. This material had small particle size, which was composed of grain size of about 100 nm. Especially, LiMn_{0.98}Y_{0.02}O₂ delivered the initial discharge capacity of about 191 mA h g⁻¹ at room temperature when cycled between 2.0 and 4.4 V vs Li/Li⁺. Moreover, it showed an excellent cycling behavior, its specific capacity remained above 173 mA h g⁻¹ after 20 cycles, and the material did not transform into spinel structure during the electrochemical cycling according to the cyclic voltammograms and X-ray powder diffraction. The electrochemical results revealed that the doping of Y³⁺ improved the performance of LiMnO₂ considerably.

Keywords Lithium battery · Cathode material · Yttrium substitution · Pillar · Cyclic voltammetry

Introduction

The layered LiMnO₂ with the O₃ (α -NaFeO₂) structure has been receiving great attention as a promising cathode material for lithium secondary batteries because of its comparatively low cost, low toxicity and high theoretical discharge capacity of 285 mA h g⁻¹, which is nearly twice as that of spinel LiMn₂O₄ [1, 2]. However, there are also some problems in utilizing the layered LiMnO₂ commercially. The major drawback of the layered LiMnO₂ is the

capacity degradation due to the phase transformation of the layered structure to spinel structure by Jahn-Teller distortion during charge-discharge cycles [2–9]. This is because the LiMnO₂ with a layered crystal structure analogous to LiCoO₂ is not thermodynamically stable but metastable [10]. To solve this problem, some research groups have tried to stabilize the layered structure by substituting Mn³⁺ by other metal ions or substituting O²⁻ by other anions; Mn-substituted LiMn_{1-y}M_yO₂ (M=Al, Cr, Co, Ni, Mg) has been widely studied [11–15]. Quine et al. [16] reported that although m-Li_xMn_{0.95}Ni_{0.05}O₂ prepared by ion exchange of NaMn_{0.95}Ni_{0.05}O₂ delivered a reversible capacity retention of 200 mA h g⁻¹ between 4.8 and 2.4 V, the material transformed slowly to a spinel-like material during cycling. Reed et al. [17] pointed out that substitution with a species that has a strong octahedral site stabilization energy such as Cr³⁺ could hinder the layered-to-spinel transformation. The collapse of a layered to a spinel structure could also be hindered by substituting larger cations in the Li layers to “pillar” the oxide; such approach has been described by Chen and Whittingham [18], for example, using K ions as the pillaring species. Meanwhile, Naghash and Lee [19] and Park et al. [20] reported that crystal structure of the material was stabilized by partial substituting fluorine or sulfur for oxygen in LiMnO₂.

Despite many transition and nontransition elements have been explored as partial substituents in place of manganese in LiMnO₂, to the best our knowledge, there is no report as of now on yttrium-substituted LiMnO₂ compound. In this paper, we have successfully synthesized LiMn_{0.98}Y_{0.02}O₂ materials through ion exchange of Li for Na from the NaMn_{0.98}Y_{0.02}O₂ precursor prepared by using rheological phase reaction method [21–25], which was a process of preparing compounds or materials from solid-liquid rheological mixture. That is, the solid reactants were fully mixed in a proper molar ratio, made up by adding a proper amount of water or other solvent to a solid-liquid rheological body in which the solid particles and liquid substance were uniformly distributed. After reaction under suitable conditions, the product was obtained. The electrochemical behaviors of the LiMn_{0.98}Y_{0.02}O₂ were studied

H. X. Zong · C. J. Cong · L. N. Wang ·
G. H. Guo · Q. Y. Liu · K. L. Zhang
Department of Chemistry, Wuhan University,
Wuhan 430072, People's Republic of China

K. L. Zhang (✉)
Centre of Nanoscience and Nanotechnology Research,
Wuhan University,
Wuhan 430072, People's Republic of China
e-mail: klzhang@whu.edu.cn
Tel.: +86-27-87218484
Fax: +86-27-68754067

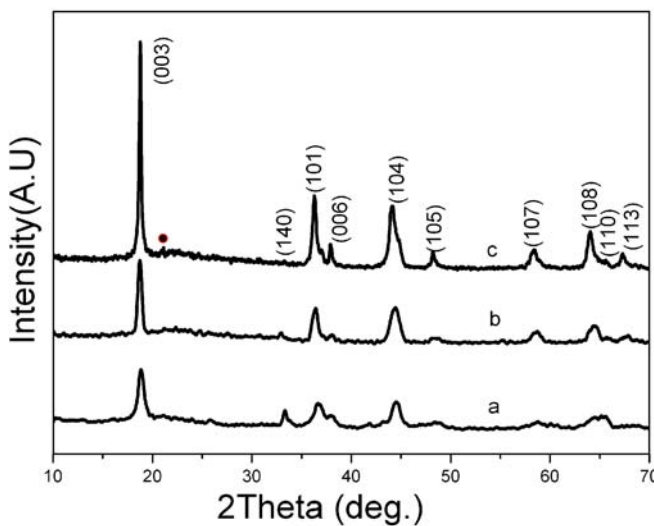


Fig. 1 X-ray diffraction (XRD) patterns of $\text{LiMn}_{0.98}\text{Y}_{0.02}\text{O}_2$ obtained at different temperatures. **a** 600°C. **b** 700°C. **c** 800°C

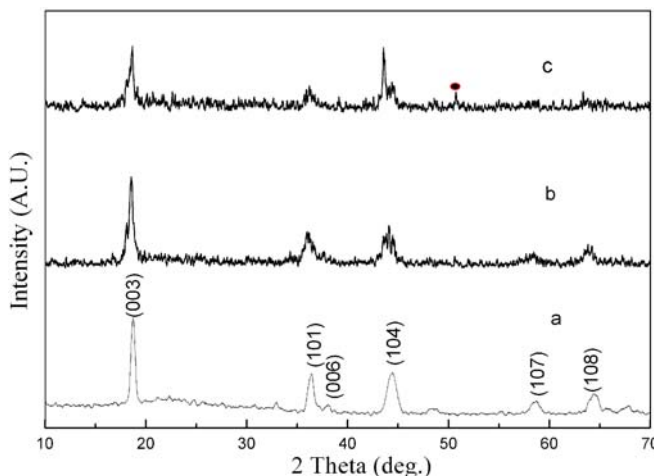


Fig. 2 XRD patterns of **a** $\text{LiMn}_{0.98}\text{Y}_{0.02}\text{O}_2$ discharged to 2.0 V after one cycle, **b** $\text{LiMn}_{0.98}\text{Y}_{0.02}\text{O}_2$ discharged to 2.0 V after 20 cycles, and **c** LiMnO_2 discharged to 2.0 V after 20 cycles

in this paper, and the electrochemical results revealed that the doping of Y^{3+} improved the performance of LiMnO_2 considerably.

Table 1 Lattice constants and real compositions of the sample measured by Rietveld analysis, inductively coupled plasma (ICP), and atomic emission spectroscopy, respectively

Sample	Lattice constants			Chemical formula
	<i>a</i> (Å)	<i>b</i> (Å)	<i>c</i> (Å)	
LiMnO_2 (700°C)	4.4958	5.7023	2.8512	$\text{Li}_{0.95}\text{Na}_{0.02}\text{MnO}_2$
$\text{LiMn}_{0.98}\text{Y}_{0.02}\text{O}_2$ (600°C)	4.5011	5.7084	2.8571	$\text{Li}_{0.93}\text{Na}_{0.03}\text{Mn}_{0.98}\text{Y}_{0.02}$
$\text{LiMn}_{0.98}\text{Y}_{0.02}\text{O}_2$ (700°C)	4.5019	5.7094	2.8598	$\text{Li}_{0.94}\text{Na}_{0.03}\text{Mn}_{0.98}\text{Y}_{0.02}$
$\text{LiMn}_{0.98}\text{Y}_{0.02}\text{O}_2$ (800°C)	4.5036	5.8011	2.8625	$\text{Li}_{0.93}\text{Na}_{0.02}\text{Mn}_{0.98}\text{Y}_{0.02}$

Experimental

Synthesis of the material

Na_2CO_3 , Mn_2O_3 (obtained by reduction of MnO_2 at 800°C for 24 h), and Y_2O_3 were mechanically mixed well in molar ratio of 1:0.98:0.02. After the powders had been ground homogeneously, a proper amount of water was added to obtain the rheological body. It reacted sufficiently to form the precursor in a container at 80–100°C for 10 h, then the mixture was dried to remove water at 120°C in air. $\text{NaMn}_{0.98}\text{Y}_{0.02}\text{O}_2$ was obtained by calcining mixture for 24 h at 600, 700, and 800°C, respectively. The prepared precursor, $\text{NaMn}_{0.98}\text{Y}_{0.02}\text{O}_2$, was introduced into a mixed solution of ethanol and LiCl . The ion exchange of sodium for $\text{NaMn}_{0.98}\text{Y}_{0.02}\text{O}_2$ with lithium was carried out at 160°C for 24 h in the mixed solution using a 50-ml Teflon-lined Parr reactor to prepare $\text{LiMn}_{0.98}\text{Y}_{0.02}\text{O}_2$. After the reaction, the solution was filtered using a vacuum suction filtering equipment, and the remaining powder was washed with distilled water. The washed powders were dried at 120°C for 12 h in a vacuum oven.

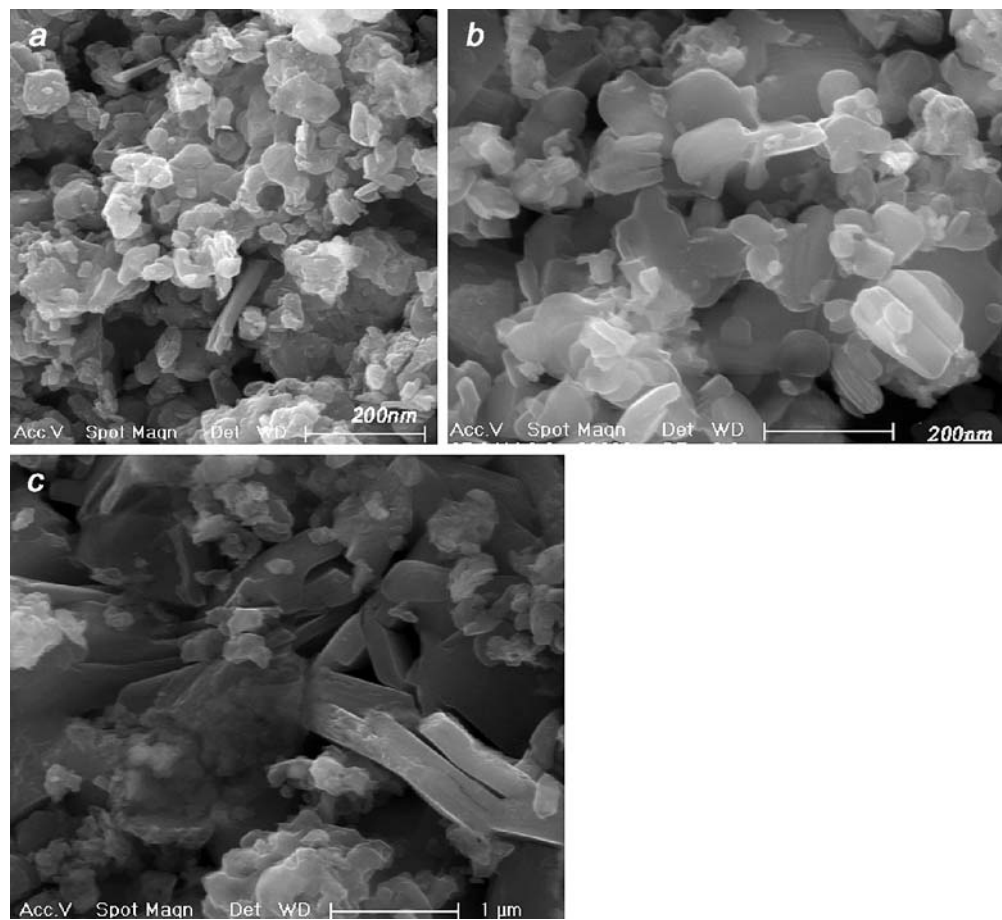
Structure determination

X-ray powder diffraction (XRD; Shimadzu XRD-6000 diffractometer with $\text{Cu K}\alpha$ radiation, $\lambda=1.54056$ Å) was carried out to understand the structure of the prepared materials. The amounts of Li, Mn, Na, and Y in the synthesized materials were analyzed with inductively coupled plasma (ICP) and atomic emission spectroscopy (ICP-AES, model IRIS, TJA, USA), respectively, to determine the real chemical composition of the materials. The grain size and morphology of the compounds were observed using a field emission scanning electron microscope (SEM). Cyclic voltammogram (CV) was employed to analyze the character of the active material. The transmission electron microscope (TEM) image was performed by means of a Joel JEM-100CX II microscope. Laser scattering (Mastersizer 2000) was used to examine the particle size and distribution of $\text{LiMn}_{0.98}\text{Y}_{0.02}\text{O}_2$.

Electrochemical testing

Test cathode electrodes consisted of 75% $\text{LiMn}_{0.98}\text{Y}_{0.02}\text{O}_2$ powders, 20% acetylene black, and 5% polytetrafluoroethylene (PTFE) by weight. Before use, the cathode elec-

Fig. 3 The scanning electron microscope photographs of $\text{LiMn}_{0.98}\text{Y}_{0.02}\text{O}_2$ prepared at **a** 600, **b** 700, and **c** 800°C



trodes must be dried at 120–130°C in a vacuum furnace for 24 h. The area of the electrode was about 1.0 cm², and the weight of active material in an electrode was about 8 mg. The cell consisted of the oxide cathode as a working electrode and lithium ribbon as a counter electrode was assembled in Ar-filled glove box. The cells filled with 1 M LiClO_4 in EC–DEC (1:1, by volume) as electrolyte were charged and discharged between 2.0 and 4.4 V (vs Li/Li⁺) using a current density of 25 mA g⁻¹ at room temperature.

Results and discussion

The XRD patterns of the $\text{LiMn}_{0.98}\text{Y}_{0.02}\text{O}_2$ obtained at different temperatures are shown in Fig. 1. All the diffraction peaks could be indexed based on a hexagonal $\alpha\text{-NaFeO}_2$ structure with a space group of $R\bar{3}m$, in which layers of lithium atoms alternate with layers containing mixtures of lithium, yttrium, and manganese atoms indicating a single-phase layered crystal structure. As the temperature increases, the intensity of peak (003) increases drastically, and the intensity of peaks (105) and (107) also increases, while the intensity of peak (104) decreases till it disappears, and the peaks (101) and (006) occur spilling. It can be seen that the crystallinity becomes better with the increase of temperature; however, when the temperature is too high, there is an impurity peak at $2\theta=21.75^\circ$, which corresponds

to Li_2MnO_3 . The X-ray diffraction patterns showed that the ion exchange is complete.

To understand the origin of superior stability of the doped $\text{LiMn}_{0.98}\text{Y}_{0.02}\text{O}_2$ compared to LiMnO_2 , XRD patterns of 20 cycled cells discharged to 2 V were compared in Fig. 2. The XRD pattern of the doped $\text{LiMn}_{0.98}\text{Y}_{0.02}\text{O}_2$ shows

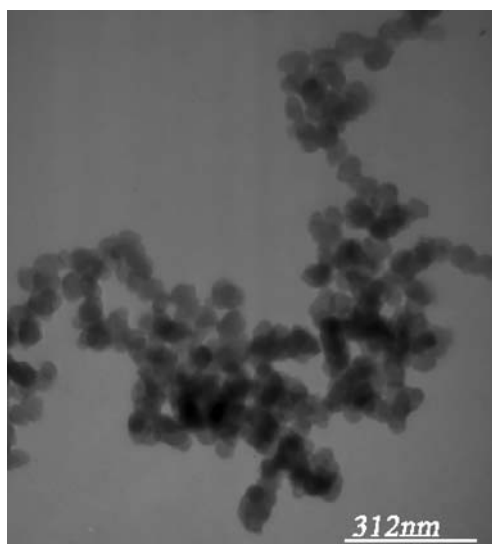


Fig. 4 Transmission electron micrograph of $\text{LiMn}_{0.98}\text{Y}_{0.02}\text{O}_2$ prepared at 700°C

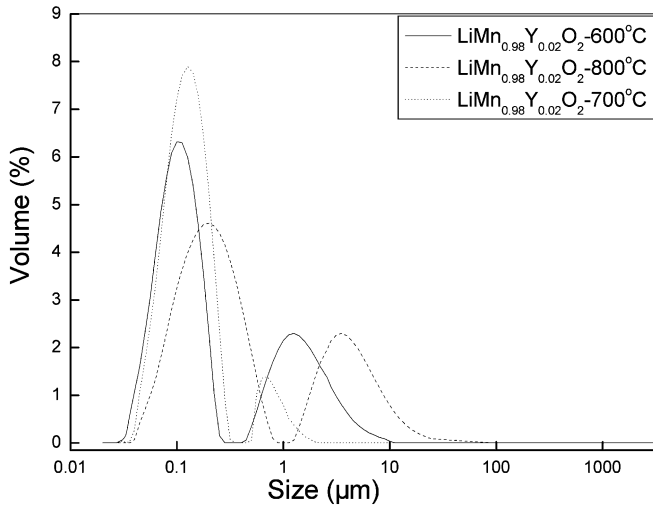


Fig. 5 The particle size distributions in volume of $\text{LiMn}_{0.98}\text{Y}_{0.02}\text{O}_2$ prepared at different temperatures

minor change after 20 cycles, but the LiMnO_2 shows bigger change after 20 cycles, especially the peaks (107) and (108) totally disappeared, and at 51.8° , a new peak appeared.

The lattice constants of LiMnO_2 (700°C) and $\text{LiMn}_{0.98}\text{Y}_{0.02}\text{O}_2$ prepared at different temperatures were calculated by the Rietveld refinement using the XRD data and real compositions are listed in Table 1. It was obvious that the lattice constants increased when doping yttrium into LiMnO_2 because the radius of Y^{3+} is larger than that of Mn^{3+} ; we deduced that doped Y^{3+} had substituted Mn^{3+} and existed in lattice structure. From Table 1, we can see that the Li element had a little loss during synthesis, but the relative content of elements (Mn and Y) is nearly the same as that of reactants. There was very little sodium in the sample, which suggested that the ion exchange was nearly complete.

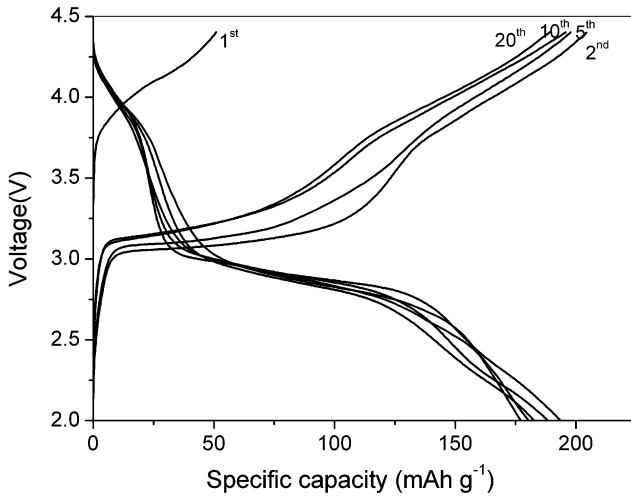


Fig. 6 Charge-discharge curves of $\text{LiMn}_{0.98}\text{Y}_{0.02}\text{O}_2$ material prepared at 700°C for 24 h in the voltage range of 2.0–4.4 V at a current density of 25 mA g^{-1} at room temperature

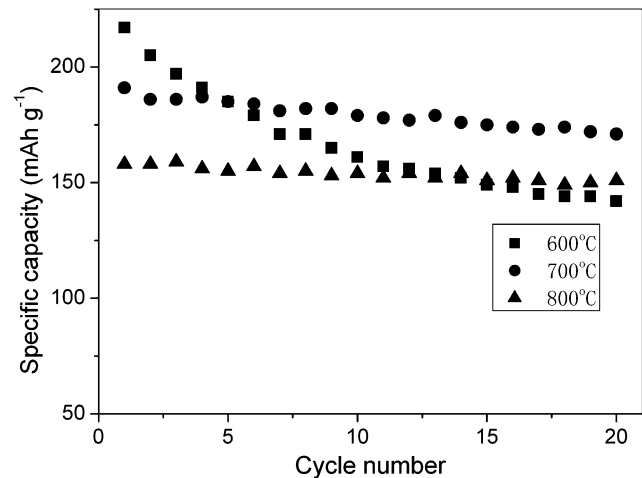


Fig. 7 Discharge capacity vs cycle number curves of the $\text{LiMn}_{0.98}\text{Y}_{0.02}\text{O}_2$ materials prepared at various temperatures for 24 h

The morphology of the powders prepared at 600, 700, and 800°C is showed in Fig. 3a-c, respectively. It is found that the sample prepared at 600°C has the smallest size and no better crystallinity, while the particle size of the sample prepared at 800°C increases dramatically, and the microstructure becomes nonuniform. The sample prepared at 700°C shows better crystallinity and smaller size; moreover, it exhibits a more uniform particle size and microstructure. By TEM, we observed both crystal shape and particle size. Fig. 4 shows that all the particle sizes are less than 100 nm and exhibits a comparative uniform particle size.

The particle size distributions (PSDs) of $\text{LiMn}_{0.98}\text{Y}_{0.02}\text{O}_2$ prepared at different temperatures are shown in Fig. 5. All the materials are characterized by a large volume distribution resulting from two populations, one centered on 0.1–0.2 μm and another around 1–5 μm . The average par-

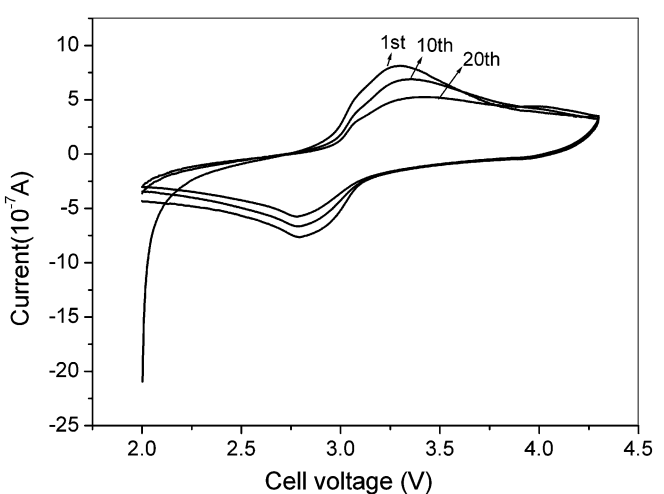


Fig. 8 Cyclic voltammograms for $\text{Li}/\text{LiMn}_{0.98}\text{Y}_{0.02}\text{O}_2$ cell obtained at scan rate of 1 mV s^{-1}

ticle size of $\text{LiMn}_{0.98}\text{Y}_{0.02}\text{O}_2$ compound prepared at 700°C is 1.02 μm , based on the experimental analysis, and most of the particle size is below 200 nm; moreover, it shows more uniform PSDs than those of the materials prepared at 600 and 800°C, which leads to predict that the compound prepared at 700°C may show better electrochemical performance.

Figure 6 shows the charge/discharge curves of the $\text{Li}/\text{LiMn}_{0.98}\text{Y}_{0.02}\text{O}_2$ cell. The first charge curve is very different from others, and its charge capacity is only about 58 mA h g^{-1} , while the discharge capacity is about 191 mA h g^{-1} , and the discharge curve exhibited a long plateau at about 2.8 V. The presence of plateau at 2.8 V is one characteristic of the m- LiMnO_2 . With further cycling, the voltage of discharge plateau shows no great change, while the voltage of the charge plateau becomes higher. It is noticeable that with further cycling, the 4-V plateau is not present, which is the characteristic of the spinel (LiMn_2O_4). The phenomenon is different from that in the previous literatures, which reported that the layered Li_xMnO_2 transformed to spinel phase during lithium ion intercalation and deintercalation [26, 27]. This reveals the structure of $\text{LiMn}_{0.98}\text{Y}_{0.02}\text{O}_2$ does not transform to spinel phase during the process of charge and discharge.

Figure 7 shows the effect of temperature on the electrochemical performance. The data demonstrated that the temperature had great influence on the initial capacity and capacity retention. The first discharge capacity decreased with the increase of temperature because the particle size increased with the increase of temperature, while the bigger size of particle means longer distance for Li^+ to diffuse and higher resistance for the material, which will result in the decrease of initial discharge capacity. The material prepared at 600°C delivered the highest discharge capacity, 218 mA h g^{-1} , at the first cycle. However, the capacity retention is the worst: the discharge capacity is only 146 mA h g^{-1} at the 20th cycle. The material prepared at 800°C showed the best capacity retention, although its capacity was the lowest, because the crystallinity and the stability of structure for the $\text{LiMn}_{0.98}\text{Y}_{0.02}\text{O}_2$ had been improved with the increase of temperature. When both higher initial capacity and capacity retention are considered, the material prepared at 700°C showed the best electrochemical performance: the first discharge capacity was 191 mA h g^{-1} and its specific capacity remained above 173 mA h g^{-1} after the 20th cycle. It is a surprise for $\text{LiMn}_{0.98}\text{Y}_{0.02}\text{O}_2$ to have both higher delivered capacity and better recharge ability as a cathode material. We speculated that three kinds of mechanism may be involved. One is that yttrium helps stabilize the open-layered structure through a pillaring effect and prevent the structure from collapsing during charge and discharge. Second is that the radius of Y^{3+} is larger than that of Mn^{3+} , which results in larger lattice parameter; thus, Li^+ ion can move more freely in the oxide and this might help increase the rate of capability. In addition, when yttrium is substituted into the LiMnO_2 , the stronger bond of Y–O (compared to Mn–O) can also improve the stability of the structure, which in turn increases the electrochemical cycleability.

Figure 8 shows the cyclic voltammograms for $\text{LiMn}_{0.98}\text{Y}_{0.02}\text{O}_2$ at a sweep range of 2.0–4.3 V. The peak current decreases gradually with cycling, the anodic peak appears at 2.8 V, and the peak voltages are stable and do no shift with cycling; on the other hand, cathodic peak appears at 3.3 V with cycling, and the peak voltage gradually shifts to higher voltage, which is consistent with the discharge plateau changing during the charge and discharge. There appears a small shoulder peak at about 4 V at the 20th cycle; however, there is no evolution of two typical spinel structures between 4.0 and 4.3 V [28, 29]. This reinforces that the structure of this material does not transform into a spinel structure with cycling.

Conclusions

A soft chemistry synthesis method, the rheological phase reaction method, has been used to synthesize $\text{LiMn}_{0.98}\text{Y}_{0.02}\text{O}_2$. The optimum synthesis temperature is 700°C. The initial discharge capacity of $\text{LiMn}_{0.98}\text{Y}_{0.02}\text{O}_2$ synthesized at 700°C is 191 mA h g^{-1} , and its specific capacity remains above 173 mA h g^{-1} after the 20th cycle. The role that yttrium plays in the LiMnO_2 has been discussed. The cyclic voltammogram studies indicate that the material does not transform into a spinel structure with cycling. Hence, it can be suggested that the $\text{LiMn}_{0.98}\text{Y}_{0.02}\text{O}_2$ material synthesized by the rheological phase reaction method can be used as a possible alternative to LiMnO_2 in response to an expanding need for advanced rechargeable lithium ion batteries.

Acknowledgement This work was supported by the National Natural Science Foundation of China (No.20071026)

References

- Capitaine F, Gravereau P, Delmas C (1996) Solid State Ion 89:197
- Park SH, Sun YK, Yoon CS, Kim CK (2002) J Mater Chem 12:3827
- Armstrong AR, Bruce PG (1996) Nature 381:499
- Horn S, Hackeray Y (1999) J Electrochem Soc 146:2404
- Armstrong AR, Dupre N, Paterson AJ, Grey CP, Bruce PG (2004) Chem Mater 16:3106
- Jang YI, Huang B, Chiang YM, Sadoway DR (1998) Electrochem Solid State Lett 1:13
- Ammundsen B, Desilvestro J, Groutso T, Hassell D, Metson JB, Regan E, Steiner R, Pickering PJ (2000) J Electrochem Soc 47:4078
- Gummow RJ, Thackeray MM (1993) J Electrochem Soc 140:3365
- Hwang SJ, Kwon CW, Portier JGC, Park HS (2002) J Phys Chem B 106:4053
- Ammundsen B, Paulsen J (2001) Adv Mater 13:12
- Robertson AD, Armstrong AR, Bruce PG (2001) Chem Mater 13:2380
- Yu LH, Yang HX, Ai XP, Cao YL (2005) J Phys Chem B 109:1148
- Patoux SB, Dolle' M, Doeff MM (2005) Chem Mater 17:1044
- Kim JH, Park CW, Sun Y-K (2003) Solid State Ion 164:43
- Hwang BJ, Tsai YW, Chen CH, Santhanam R (2003) J Mater Chem 13:1962
- Quine TE, Duncan MJ, Armstrong AR, Robertson AD, Bruce PG (2000) J Mater Chem 10:2838

17. Reed J, Ven VD, Ceder G (2000) In: Abstracts of the 198th meeting of the Electrochemical Society, Phoenix, p 174
18. Chen R, Whittingham MS (1997) *J Electrochem Soc* 144:64
19. Naghash AR, Lee JY (2001) *Electrochim Acta* 46:2293
20. Park SH, Lee JY, Sun YK (2003) *Electrochim Commun* 5:123
21. Zhang Y (2002) *Chem Lett* 2:176
22. Sun JT (1999) *Mater Sci Eng B* 64:157
23. Tang H (2002) *Chem Lett* 8:822
24. Yuan LJ (2004) *Inorg Chim Acta* 357:89
25. Yin MC (2004) *Polyhedron* 23:529
26. Vitins G, West K (1997) *J Electrochem Soc* 144:2587
27. Park SH, Lee YS, Sun YK (2003) *Electrochim Commun* 5:124–128
28. Rahner D, Machill S, SchloÈH, Siury K, Kloss M, Plieth W (1998) *J Solid State Electrochem* 2:78
29. Wang GG, Wang JM, Mao WQ, Shao HB, Zhang JQ (2005) *J Solid State Electrochem* 9:524